OPEN ACCESS

University of BRISTOL

Peer reviewed version

Link to published version (if available):
10.1021/jp501517t

Link to publication record in Explore Bristol Research
PDF-document

Quantum Yields for Photochemical Production of NO_2 from Organic Nitrates at Tropospherically Relevant Wavelengths

Christina M. Higgins, Louise A. Evans, Guy C. Lloyd-Jones[#], Dudley E. Shallcross, David P. Tew, and Andrew J. Orr-Ewing*

School of Chemistry, University of Bristol, Cantock's Close, Bristol BS8 1TS, UK

[#] *School of Chemistry, University of Edinburgh, West Mains Road, Edinburgh EH9 3JJ*

* Author for correspondence

 e-mail: a.orr-ewing@bristol.ac.uk

 Tel: +44 (0)117 9287672

Abstract

Absorption cross sections and quantum yields for NO_2 production (Φ_{NO_2}) are reported for gaseous methyl, ethyl, n-propyl and isopropyl nitrate at 294 K. Absorption cross sections in the wavelength range 240 – 320 nm agree well with prior determinations. NO_2 quantum yields at photo-excitation wavelengths of 290, 295 and 315 nm are unity within experimental uncertainties for all the alkyl nitrates studied, and are independent of bath gas (N_2) pressure for total sample pressures in the range 250 – 700 Torr. When averaged over all wavelengths and sample pressures, values of Φ_{NO_2} are 1.03 ± 0.05 (methyl nitrate), 0.98 ± 0.09 (ethyl nitrate), 1.01 ± 0.04 (n-propyl nitrate) and 1.00 ± 0.05 (isopropyl nitrate), with uncertainties corresponding to 1 standard deviation. Absorption cross sections for ethyl nitrate, isopropyl nitrate and two unsaturated dinitrate compounds, but-3-ene-1,2-diyl dinitrate and (Z)-but-2-ene-1,4-diyl dinitrate in acetonitrile solution are compared to gas-phase values, and over the wavelength range 260 – 315 nm, the gas-phase values are well reproduced by dividing the liquid phase cross sections by 2.0,1.6, 1.7 and 2.2 respectively. Reasonable estimates of the gas-phase absorption cross sections for low volatility organic nitrates can therefore be obtained by halving the values for acetonitrile solutions. The quantum yield for NO_2 formation from photoexcitation of but-3-ene-1,2-diyl dinitrate at 290 nm is significantly lower than those for the alkyl (mono) nitrates: a best estimate of $\Phi_{NO_2} \leq 0.25$ is obtained from the experimental measurements.

Keywords: organic nitrate, photochemistry, tropospheric chemistry, quantum yield, cavity ring-down spectroscopy

1. Introduction

Growing interest in the atmospheric photochemistry of organic nitrate ($RONO_2$) species reflects their important role in tropospheric oxidation pathways.[1-4] Primary sources of tropospheric $RONO_2$ include direct emissions from the oceans and from biomass burning.[5-6] Secondary formation of $RONO_2$ results from the daytime photo-oxidation of hydrocarbons in the presence of NO, or night-time reaction of unsaturated hydrocarbons with NO_3, as part of the coupled HO_x and NO_x catalytic cycles.[2, 7] $RONO_2$ species have relatively long atmospheric lifetimes so can be transported over large distances in the troposphere,[8] and have the potential to release or sequester NO_2 in the atmosphere. NO_2 is a key constituent of the ozone cycle since its photolysis is part of the only known formation pathway of tropospheric ozone. In an urban modelling study, Farmer *et al.* highlighted the potential reduction in the formation of ozone resulting from the photochemical production of organic nitrates, which terminate the HO_x and NO_x cycles leading to NO_2.[9] The formation of $RONO_2$ not only sequesters NO_x but also inhibits the production of RO radicals which would further react to form other oxygenated species.

Difunctional organic nitrate compounds can form when NO_3 reacts with unsaturated hydrocarbons in air, and the chemistry of these processes was discussed by Barnes *et al.*[10] Reaction of NO_3 with isoprene is an important example,[11] producing products such as nitrooxy carbonyls and, in principle, organic dinitrate species. For example, in a chamber study, Rollins *et al.*[12] observed dinitrate species produced in the reaction of primary isoprene nitrates with NO_3.

The main removal mechanism for alkyl nitrates in the troposphere is either oxidation via reaction with OH (for $RONO_2$ with a carbon number ≥ 5) or via photolysis (for smaller $RONO_2$).[13-15] Photochemical destruction of $RONO_2$,

$$RONO_2 + h\nu \rightarrow RO + NO_2 \qquad\qquad (1)$$

releases NO_x into the atmosphere and thus contributes to further propagation of the HO_x and NO_x cycles. $RONO_2$ photolysis to liberate NO_2 is generally assumed to occur with quantum yield (Φ_{NO_2}) values of unity,[2-3, 13, 16-18] but to date there has been only limited experimental verification. [3, 15, 19-22] Here, we focus on measurements of quantum yields for NO_2 from process (1) following photo-excitation of $RONO_2$ at UV wavelengths appropriate for the

Earth's troposphere ($\lambda \geq 290$ nm). At these wavelengths, absorptions occur via weak $\pi^* \leftarrow n$ transitions centred on the $-ONO_2$ group, and the spectral bands extend to wavelengths around 330 nm. We also report UV absorption cross sections, and compare gas-phase absorption spectra with those for liquid solutions of the nitrates.

The organic nitrate compounds studied are shown in figure 1, and include two dinitrate compounds: but-3-ene-1,2-diyl dinitrate (or 3,4-dinitrooxy-1-butene [7]) and (Z)-but-2-ene-1,4-diyl dinitrate (or cis 1,4-dinitrooxy-2-butene [7]). For convenience, these two compounds are henceforth referred to as dinitrates A and B respectively.
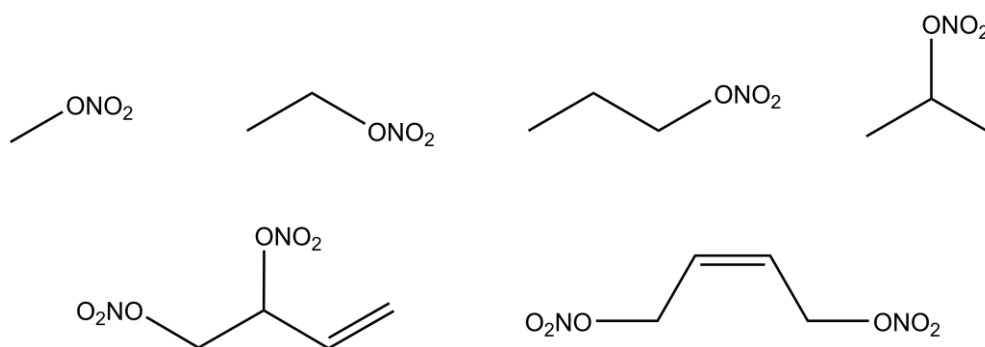
Figure 1: The organic nitrate compounds chosen for the current study. Top row: methyl, ethyl, n-propyl and isopropyl nitrate. Bottom row: dinitrate A (but-3-ene-1,2-diyl dinitrate) and dinitrate B ((Z)-but-2-ene-1,4-diyl dinitrate).

2. Experimental

Although isopropyl nitrate is commercially available (Fluka, 99.99%), the other organic nitrates shown in figure 1 needed to be synthesized for photochemical studies. Section 2.1 describes the synthetic methodology and the procedures used to ensure high purity of the required compounds. Sections 2.2 and 2.3 respectively summarize the experimental methods for measurement of absorption cross sections and photochemical NO_2 quantum yields.

3

2.1 Synthesis of Organic Nitrates

Methyl nitrate was synthesised using a method described by Blatt.[23] The syntheses of the other nitrate compounds are described below.

Ethyl nitrate: Bromoethane (5 mL, 66.7 mmol) was added dropwise to a cooled, stirring solution of silver nitrate (11.3 g, 66.4 mmol) in benzonitrile (7.5 mL) in the absence of light. After 24 hours the reaction had proceeded to completion, as indicated by ^{1}H NMR, and was filtered through a pad of Celite. The product was isolated as a colourless oil following distillation (oil-bath at 140 °C, 2.97 g, 50 %).

n-propyl nitrate: 1-Bromopropane (5 mL, 55.0 mmol) was added dropwise to a cooled, stirring solution of silver nitrate (9.50 g, 56.0 mmol) in benzonitrile (7.5 mL) in the absence of light. After 24 hours the reaction had proceeded to completion, as indicated by ^{1}H NMR, and was filtered through a pad of Celite. The product was isolated as a colourless oil following distillation (oil-bath at 140 °C, 2.31 g, 40 %).

Dinitrate A: 3,4-Dichloro-1-butene (5 mL, 46 mmol) was added dropwise to a cooled, stirring solution of silver nitrate (27.4 g, 161.0 mmol) in acetonitrile (40 mL) in the absence of light. The reaction was monitored by ^{1}H NMR until complete (24 – 36 h), at which time the suspension was filtered through a pad of Celite. Flash column chromatography (silica, hexanes/EtOAc 9:1) gave the desired product as a colourless oil (R_f = 0.39, 1.73 g, 21 %) and an isomer, identified as *trans*-1,4-dinitrooxy-2-butene, as a colourless oil (R_f = 0.15, 2.24 g, 27 %). ^{1}H and ^{13}C NMR demonstrated that the dinitrate A samples were >99% pure.

Dinitrate B: *cis*-1,4-Dichloro-2-butene (5 mL, 47.5 mmol) was added dropwise to a cooled, stirring solution of silver nitrate (21.2 g, 125.0 mmol) in acetonitrile (40 mL) in the absence of light. The reaction was monitored by ^{1}H NMR until complete (24 – 36 h), at which time the suspension was filtered through a pad of Celite. Flash column chromatography (silica, hexanes/EtOAc 9:1) gave the desired product as a colourless oil (6.62 g, 78 %). NMR analysis confirmed <3% of the E-isomer.

Sample verification was carried out using IR and NMR spectroscopy (with outcomes reported in the Supplementary Information). The samples were stored in the dark in a fridge until required for use, and were found to be stable over several months under these conditions, as

confirmed by periodic tests by ^{1}H NMR. The ChemSpider database[24] lists the following vapour pressures for the organic nitrate compounds at 298 K: methyl nitrate, 217 Torr; ethyl nitrate, 75 Torr; isopropyl nitrate, 44 Torr; n-propyl nitrate, 27 Torr; dinitrate A, 0.2 Torr; dinitrate B, 0.02 Torr.

2.2 Absorption Cross Sections

All the nitrate compounds shown in figure 1 are liquids at room temperature and pressure, and the dinitrates have very low vapour pressures making study of their gas phase spectroscopy and photochemistry challenging. Gas phase absorption spectra were successfully measured for the methyl, ethyl, n-propyl and isopropyl nitrate at various vapour pressures using an Ocean Optics USB UV/Vis spectrometer. A custom-made gas absorption cell was built to facilitate study of low vapour pressure organic nitrates. The gas cell was 13 cm in length with a diameter of 1.5 cm. Removable quartz windows allowed cleaning of all internal surfaces of the cell between samples to prevent cross-contamination. The cell was designed with two side-arms: one allowed flow of gases into the cell, and a $0 - 10$ Torr calibrated capacitance manometer was attached to the other for in-cell monitoring of sample pressures. The gas cell was attached to a glass vacuum line on which $RONO_2$ samples were handled. Fibre-optic cables delivered light to the cell from a UV lamp, and collected transmitted light for analysis by the spectrometer. In this way, the cell remained static during all measurements, so that background losses from the cell windows and optical fibres were constant and could be accurately subtracted from measurements made with the sample vapour present. Spectra were recorded using the SpectraSuite spectroscopy software that controlled the Ocean Optics spectrometer. For each alkyl nitrate, spectra of the vapour were recorded for an average of 4 pressures from $1.5 - 17$ Torr with at least three scans per pressure.

Despite the design of sample cell and vacuum line described previously, the vapour pressures of the dinitrates proved to be too low for reliable determination of UV absorption spectra in the 13-cm long sample cell. Therefore, we obtained absorption spectra of liquid samples at concentrations of $0.08 - 0.60$ M in solution in acetonitrile. Absorption measurements were made in a quartz cuvette with a pathlength of 0.1 cm and used the same spectrometer as the gas-phase samples. Similar measurements were made for the more volatile alkyl nitrates so that direct comparisons could be made between the gas and solution phase spectra.

2.3 Quantum Yield Determinations

The experimental apparatus used for absolute determination of NO_2 quantum yields has been described in detail previously, and only a summary is presented here. Two separate laser systems were used: the first generated tunable UV light pulses for photodissociation of $RONO_2$, and the second produced a pulsed beam for cavity ring-down spectroscopy (CRDS) detection of the NO_2 photofragment in the visible region of the spectrum. The photolysis beam was generated from the output of a dye laser (Sirah Cobra Stretch) pumped by the second harmonic (532 nm) of a Nd:YAG laser (Continuum Surelite III). In the amplifier section of the dye laser, the light passed through a Bethune cell to create a uniform circular beam. The visible light from the dye laser was frequency doubled by a KDP crystal, giving 1.0 – 1.5 mJ of energy per UV pulse at wavelengths from 290 – 315 nm. The UV beam entered and exited the sample flow tube via fused silica windows attached to the sides of the flow tube. The photolysis laser was triggered at 0.5 Hz to allow replenishment of the gas sample in the flow tube between UV pulses.

The wavelength of the probe laser was fixed at λ=439.2 nm, for detection of NO_2 photoproducts via the $A^2 B_2 - X^2 A_1$ electronic transition. No interfering absorptions were expected from the parent $RONO_2$ or other photoproducts. To generate the blue probe light, a second dye laser (Cobra, Sirah) was pumped by the third harmonic (355 nm) of a Nd:YAG laser (Continuum Surelite). The dye laser had oscillator and pre-amplifier stages, but no further amplification stage, and gave an output of ~2 mJ per pulse. The laser beam was attenuated by a neutral density filter to prevent saturation in absorption measurements.

The $RONO_2$ sample flowed through a glass tube, the ends of which were adapted to hold high-reflectivity mirrors (R = 0.99998 at 440 nm, Los Gatos Research) to form a ring-down cavity (RDC) required for CRDS detection of NO_2. The UV photolysis beam crossed the RDC at 90° to the cavity axis: depending on UV wavelength, either a single or (spatially offset) double pass of the photolysis beam was used. Double passing was most necessary for photolysis at 315 nm, where the $RONO_2$ absorption cross sections are very small. The photolysis and probe laser beams were reproducibly overlapped with the aid of a removable tool containing carefully machined alignment apertures. A 30 μs time delay was set between the photolysis and probe laser beams to ensure optimum NO_2 signal.[19]

RONO$_2$ samples were prepared as the vapour of the organic nitrate diluted in nitrogen in 5-litre glass bulbs. All the RONO$_2$ compounds used were liquids at room temperature. The vapour pressures of the alkyl nitrates were high enough that sample preparation was straightforward. Sample bulbs were filled on a glass vacuum line by allowing a given pressure of RONO$_2$ gas (typically 1 – 15 Torr) to flow into an empty 5-litre bulb followed by addition of nitrogen to a specific total pressure (typically 300 – 760 Torr). However, modified procedures were adopted to prepare samples of the lower volatility dinitrates, which were stored in glass fingers attached to the glass bulbs to encourage complete equilibration of the liquid and vapour in a volume sufficient for flow experiments. All sample bulbs were wrapped in black plastic to minimise any possible degradation from light sources. The sample bulbs were made at least an hour before experimental use to ensure mixing of the two gases. Constant flow conditions were maintained by metering valves placed between the sample bulb and the flow tube, and between the flow tube and a rotary pump. Under typical conditions of sample flow, ring-down times were τ~35 μs, compared to an empty cavity ring-down time $\tau_0 = 44$ μs, indicating trace ($\leq 10^{-5}$ Torr) contamination of the RONO$_2$/N$_2$ samples by NO$_2$.

3. Results and Discussion

Both absorption cross sections and NO$_2$ quantum yields are required for atmospheric models of photochemical rates of removal of organic nitrates. The focus of the current work is on wavelengths longer than 290 nm, where absorption by the nitrate compounds is weak, but the solar flux in the troposphere rises with increasing wavelength. Absorption cross section data are presented to wavelengths as short as 240 nm, but quantum yield measurements were made at single selected wavelengths of 290, 295 and 315 nm.

3.1 Absorption Cross Sections

Figure 2 shows the results of absorption cross section measurements for four alkyl nitrates: methyl, ethyl, n-propyl and isopropyl nitrate. The data were obtained using the 13-cm pathlength gas cell described in section 2, at a temperature of 294 K. Spectra were recorded typically for 4 different pressures of each alkyl nitrate from 1.5 – 17 Torr, with at least three scans per pressure, and the absorption cross sections plotted are the averages of values
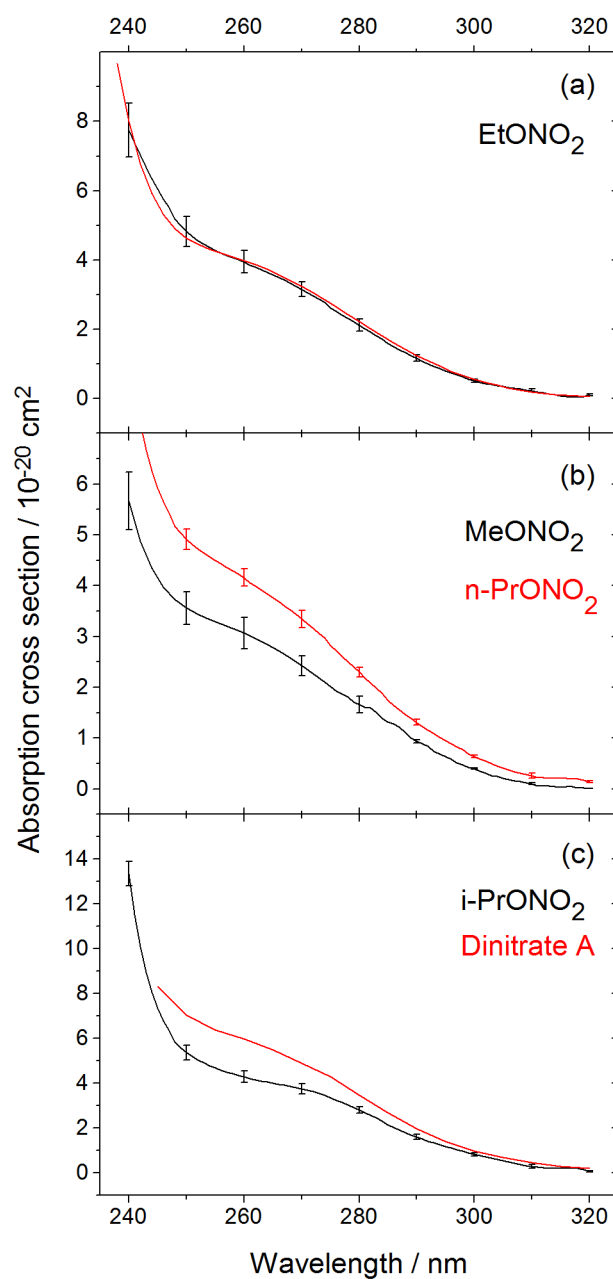
Figure 2: Averaged absorption cross-section data for gaseous organic nitrates: (a) ethyl nitrate from the current work (black) and reference [15] (red); (b) methyl nitrate (black) and n-propyl nitrate (red); (c) isopropyl nitrate (black) and dinitrate A (red), with the latter spectrum from reference [7]. All spectra from the current study were recorded at a temperature of 294 K.

derived from these measurements. To determine uncertainties in the absorption cross sections, linear fits were made to the absorbance, obtained at 10 nm wavelength intervals, as a function of $RONO_2$ sample pressure. The uncertainties shown in figure 2 are 1 standard deviation (SD) of the gradients of these fits at each chosen wavelength. For wavelengths from 240 to 300 nm, the uncertainties were 3 - 10 %, and at wavelengths $\geq$ 310 nm, the uncertainties were $\leq$ 28 %. The increase in uncertainties at longer wavelengths derives from a combination of weak absorption and use of low pressure samples. The data plotted in figure 2 are tabulated in Supplementary Information.

Figure 2 compares the measurements with a prior determination by Talukdar *et al.*[15] for ethyl nitrate. The figure also includes a plot of the wavelength-dependent cross sections reported by Barnes *et al*. for dinitrate A.[7] The alkyl nitrate absorption cross-sections are in good agreement with previously published values.[3, 13, 15, 21-22, 25-26] As the size of the alkyl group and the degree of branching increase, so do the absorption cross-sections. This trend is well documented and is attributed to donation of electron density to the ONO_2 chromophore and to steric influence on the ONO bond angle.[27-28] The trend is nonlinear in the alkyl chain length because the inductive effect is most pronounced over distances of two to three carbon atoms.[13] An analogous increase of absorption cross-section with size of the alkyl group has also been reported for liquid phase spectra of alkyl nitrates.[27]

The vapour pressures of dinitrates A and B proved to be too low for satisfactory absorption cross section measurements to be made for gaseous samples in the 13-cm pathlength cell. We therefore explored whether liquid phase spectra might be used to predict reliably the gas phase absorption spectra. Absorption spectra were measured for $0.08 - 0.60$ M solutions of ethyl nitrate, isopropyl nitrate and the two dinitrate species in acetonitrile using a quartz cuvette with an optical pathlength of 0.1 cm. Acetonitrile was chosen because it is a good solvent for the organic nitrates, is unreactive with them, and shows negligible absorption in the wavelength region of interest. Absorbances determined at 5-nm intervals in the wavelength range $240 - 325$ nm, were plotted against concentration for each $RONO_2$ to obtain molar extinction coefficients, ε (M^{-1} cm^{-1}). These extinction coefficients were then converted to absorption cross-sections. At 290 nm, 1 SD uncertainties in the absorption cross sections were 17, 4, 5 and 2 % for ethyl nitrate, isopropyl nitrate, dinitrate A and dinitrate B, respectively. The larger uncertainty for the ethyl nitrate may be a consequence of some sample degradation prior to the measurements.

9

Csizmadia *et al.*[27] determined extinction coefficients for various alkyl nitrates dissolved in heptane, and the extinction coefficients we observed for acetonitrile solutions are in reasonable agreement with this earlier study. For example, the current and previous measurements for ethyl nitrate give respective extinction coefficients of 2.7 and 2.0 M^{-1} cm^{-1} at 300 nm, 9.8 and 7.0 M^{-1} cm^{-1} at 280 nm, and 18.5 and 14.0 M^{-1} cm^{-1} at 260 nm. Similarly for isopropyl nitrate, the respective extinction coefficients are 3.0 and 3.0 M^{-1} cm^{-1} at 300 nm, 12.3 and 10.0 M^{-1} cm^{-1} at 280 nm, and 23.0 and 19.0 M^{-1} cm^{-1} at 260 nm.

Figure 3 compares spectra of the solutions of organic nitrates in acetonitrile (scaled as discussed below) with gas phase spectra. For dinitrates A and B, gas-phase absorption cross-section data were obtained from Barnes *et al.*[7] The spectra show (at most) only weak solvent shifts. For all four organic nitrates, absorption cross sections are larger for the liquid solutions than for the gas-phase samples, and division of spectra for the two phases (liquid / gas phase) over the wavelength range 260 – 315 nm gives ratios (with 1 SD uncertainties) of 2.0 ± 0.5, 1.6 ± 0.3, 1.7 ± 0.1 and 2.2 ± 0.7 for ethyl nitrate, isopropyl nitrate, dinitrate A and dinitrate B, respectively. In the case of dinitrate B, a systematic change in the ratio indicates a small solvent shift of the absorption band, and there is a similar but weaker trend for isopropyl nitrate. Spectra of the organic nitrates in solution were scaled by these ratios to allow the comparison of absorption bands shown in figure 3. The comparisons made in figure 3 suggest that the gas phase absorption cross sections of low volatility organic nitrates can be reliably estimated in the $\lambda \geq 290$ nm wavelength range by dividing the solution phase spectra (obtained in acetonitrile) by a factor of 2.
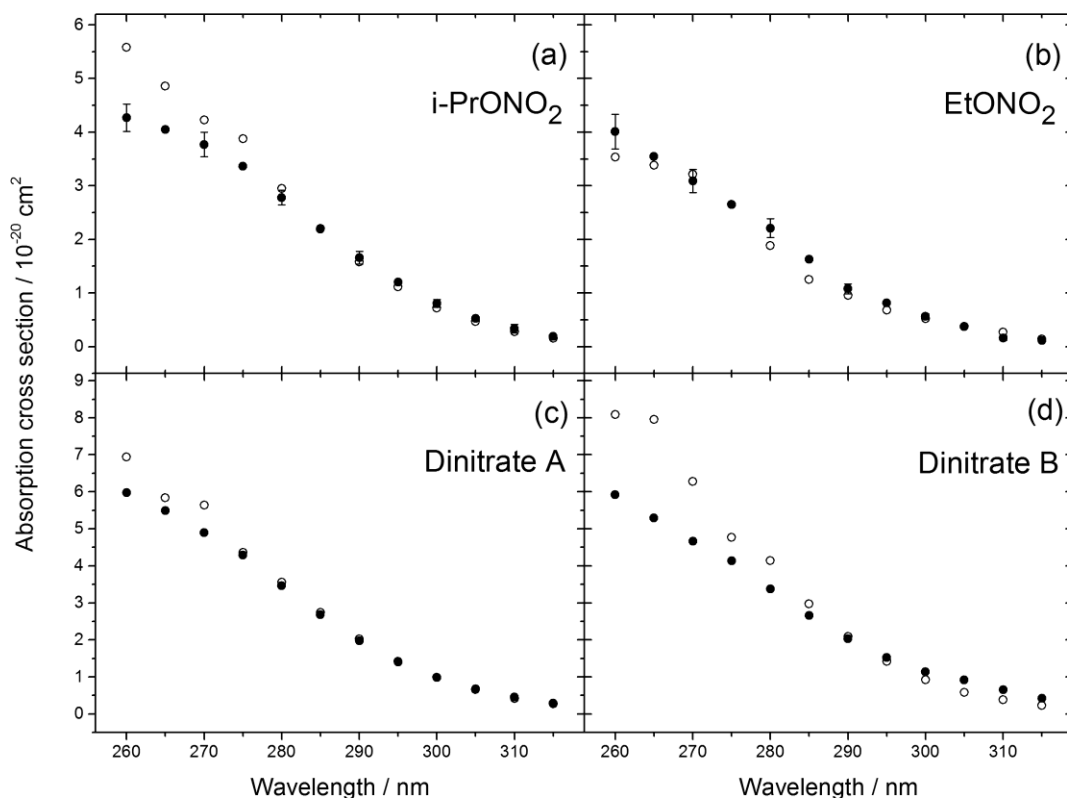
Figure 3: Absorption spectra of: (a) isopropyl nitrate; (b) ethyl nitrate; (c) dinitrate A; (d) dinitrate B. Black filled circles are gas-phase data and open circles are derived from solutions of the organic nitrates in acetonitrile, with rescaling of the absorption cross sections by division by constant factors close to 2 as described in the main text. Gas-phase data for dinitrates A and B are taken from reference [7].

3.2 NO$_2$ Quantum Yields

NO$_2$ quantum yields, Φ_{NO_2}, were determined for the four alkyl nitrates at selected photolysis wavelengths and total sample pressures. The analysis used to derive NO$_2$ quantum yields from experimentally observed differences in ring-down rate coefficients, Δk, with and without the photolysis laser, was described previously by Gorrotxategi Carbajo and Orr-Ewing.[19] For a single pass of a photolysis laser beam with elliptical Gaussian intensity profile and beam waists along the principal ellipse axes x and y of w_x and w_y, Δk is given by:

11

$$\Delta k = \frac{c\, N_{ph} \Phi_{NO_2} \sigma_{NO_2}}{L w_x \ell} \sqrt{\frac{2}{\pi}} \{1 - exp(-\sigma_{RONO_2} n_{RONO_2} \ell)\} \qquad (2)$$

In equation (2), n_{RONO_2} is the number density of the parent organic nitrate, which has an absorption cross section σ_{RONO_2} at the UV wavelength of the photolysis laser. NO_2 is detected at 439.2 nm, with an absorption cross section σ_{NO_2} from Vandaele $et\ al.$[29] (with RMS uncertainty of 3.2%). A UV pulse from the photolysis laser containing N_{ph} photons (with ≤5% precision[19]) propagates through the sample for a distance ℓ (with ≤3% uncertainty) along the z direction, orthogonal to the axis of the ring-down cavity, which defines the y direction. The linear ring-down cavity is constructed from two mirrors separated by a distance L, and c denotes the speed of light. Accounting for double-passing of the photolysis laser beam through the sample is straightforward if allowance is made for loss of UV pulse energy in the additional optics in the extended beam path. Choice of experimental conditions controlled the values of parameters n_{RONO_2} and N_{ph}, and the photolysis laser beam waists were determined precisely by measurement of the Gaussian intensity profiles across the laser beam in horizontal and vertical directions. Beam waist values for different UV laser wavelengths used in the experiments are tabulated in the Supplementary Information and were measured with a precision of ≤ 3 % (1 SD). Reference 19 provides further discussion of sources of experimental uncertainty.

Datasets typically consisted of 2000 data points, of which 1900 were background measurements without the photolysis laser and 100 were measurements with the photolysis laser firing. Figure 4 shows portions of such datasets for four different organic nitrates. Baseline fluctuations are most likely a consequence of trace amounts of NO_2 in the organic nitrate samples, and the resultant uncertainty in determination of the ring-down time (when averaged over a full dataset) was 1-2%. At least 3 datasets were accumulated for each $RONO_2$ sample in the ring-down cavity, so ≥ 300 determinations of NO_2 absorption were made per quantum yield value derived from data analysis. A calibrated power meter measured UV photolysis energies, which were chosen to be from 0.6 − 1.2 mJ per pulse. Alkyl nitrate partial pressures were selected in the range 7 − 10 Torr, 2 − 6 Torr and 2 − 5 Torr for photolysis wavelengths of 315 nm, 295 nm and 290 nm, respectively. Isopropyl nitrate has a known quantum yield of unity from prior measurements,[19] so this species was

used as a check of the experimental procedures. However, all Φ_{NO_2} values reported here derive directly from experimental measurements without any correction.
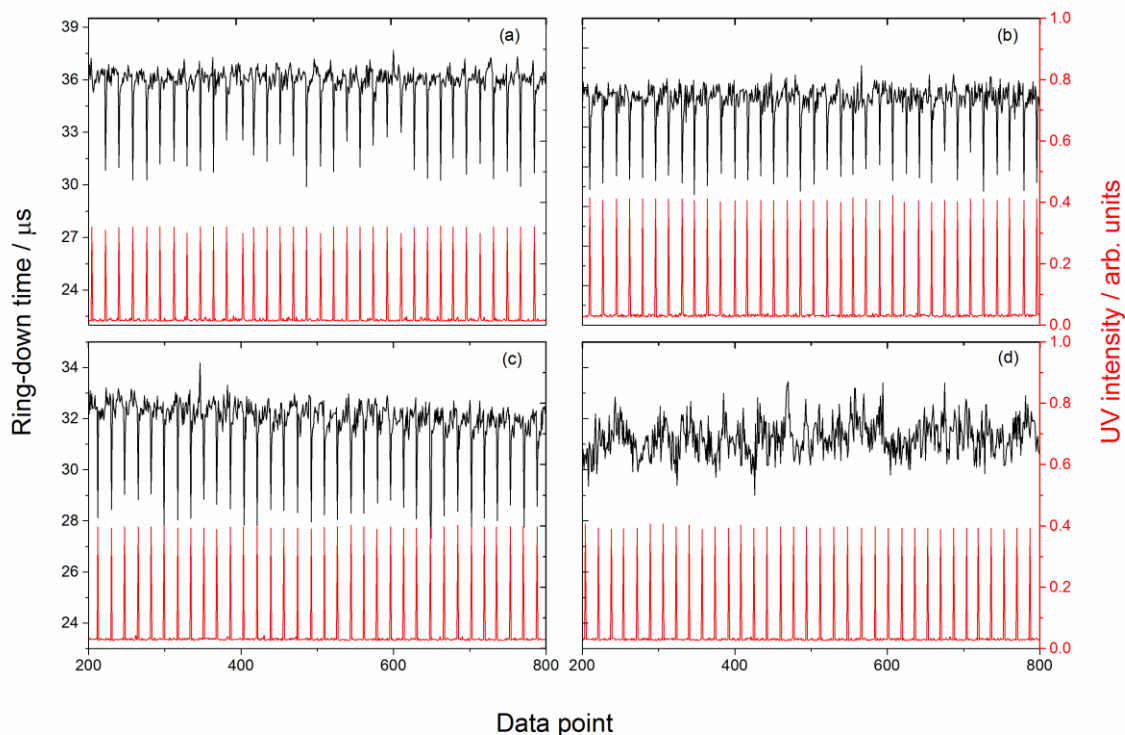

Figure 4: Unprocessed partial datasets for (a) methyl nitrate, (b) ethyl nitrate, (c) isopropyl nitrate and (d) dinitrate A, for photolysis at 290 nm with a total sample pressure of 500 Torr and ~1 mJ per pulse of UV energy. The red lines (with right-hand axis) show UV photolysis laser intensity, with positive going spikes corresponding to points at which the laser fired. The black lines (with left-hand axis) show ring-down times without and with the photolysis laser. Negative going spikes indicate NO_2 formation.

The datasets shown in figure 4 were obtained for partial pressures of ~5 Torr for the methyl, ethyl and isopropyl nitrates. The vapour pressure of dinitrate A limited experiments to a lower partial pressure of ~1 Torr, but this difference cannot solely account for the much weaker NO_2 signals in data such as those shown in figure 4 for two reasons. Firstly, corresponding experiments with 1 Torr of isopropyl nitrate showed more pronounced drops in the ring-down time (and thus NO_2 formation) synchronous with pulses in the UV laser. Secondly, the absorption cross sections for the dinitrates are larger than for mononitrates.

13

Furthermore, the presence of dinitrate A in the ring-down cavity was verified by collecting some of the flowing gas sample into an evacuated cell and measuring its IR absorption spectrum. From the average of three photolysis datasets for dinitrate A, we estimate an upper limit to the NO_2 photolysis quantum yield at 290 nm of $\Phi_{NO_2} \leq 0.25$. Table 1 displays all the derived quantum yields for photolytic NO_2 production from various organic nitrates at different photolysis laser wavelengths and sample pressures. In all cases, the bath gas used was N_2 and was in considerable excess over the organic nitrate. The quoted precisions in Φ_{NO_2} are 1 SD, and include propagation of uncertainties from the $RONO_2$ and NO_2 absorption cross-section values and from other key experimental parameters, as well as variation in individual Φ_{NO_2} determinations from separate datasets at a given total pressure and photolysis wavelength.

Table 1: NO_2 Quantum Yields and Organic Nitrate Absorption Cross Sections at Selected UV Wavelengths and at Different Total Sample Pressures. Absorption cross sections were obtained either from the current study or from the references shown in the final column (for 315-nm photolysis only). Sources of uncertainty are discussed in the main text and specified errors are 1 SD.

Nitrate Compound and Photolysis Wavelength	NO₂ Quantum Yield			Absorption Cross Section / 10^{-20} cm² molecule^{-1}
	250 Torr	500 Torr	700 Torr	
Isopropyl Nitrate				
315 nm		0.97 ± 0.12		0.170 ± 0.009 [15]
295 nm	1.06 ± 0.12	0.96 ± 0.12	0.95 ± 0.13	1.20 ± 0.10
290 nm	1.01 ± 0.12	1.03 ± 0.13	1.03 ± 0.12	1.66 ± 0.12
n-Propyl Nitrate				

295 nm	0.99 ± 0.09	0.96 ± 0.15	1.02 ± 0.09	0.989 ± 0.04
290 nm	1.01 ± 0.15	1.02 ± 0.10	1.03 ± 0.09	1.35 ± 0.05
Ethyl Nitrate				
290 nm	0.97 ± 0.20	1.01 ± 0.17	0.96 ± 0.13	1.08 ± 0.11
Methyl Nitrate				
315 nm		0.96 ± 0.11		0.0636 ± 0.0032 [15]
290 nm	1.1 ± 0.09	1.03 ± 0.09	1.02 ± 0.10	0.89 ± 0.04
Dinitrate A				
290 nm		≤ 0.25		1.98 ± 0.50 [7]

The majority of prior determinations of quantum yields for alkyl nitrates were made at photolysis wavelengths of 248 and 308 nm (corresponding to emission wavelengths of excimer lasers). However, Gorrotxategi Carbajo and Orr-Ewing reported Φ_{NO_2} values for methyl and isopropyl nitrate at photolysis wavelengths of 308, 315 and 320 nm.[19] At total pressures of 500 Torr and 700 Torr, quantum yields were the same (within experimental uncertainties), but lower quantum yield values were reported at a pressure of 200 Torr for experimental conditions similar to those used in the current study. For example, for methyl nitrate, Φ_{NO_2} values were 1.01 ± 0.05 (at 700 Torr total pressure) and 1.00 ± 0.09 (500 Torr), respectively, but at 200 Torr, Φ_{NO_2} = 0.72 ± 0.07. A similar trend was observed for isopropyl nitrate, Φ_{NO_2} = 1.01 ± 0.05 (700 Torr), 1.00 ± 0.06 (500 Torr) and 0.72 ± 0.05 (200 Torr). The suggestion was made that the NO_2 formed in vibrationally excited levels,[19, 30] and quenching by the N_2 bath gas was necessary for accurate Φ_{NO_2} determinations. However, no such pressure dependence of Φ_{NO_2} is seen in the current work, with quantum yields of unity

even at total pressures of 250 Torr, suggesting that the NO_2 is fully equilibrated when probed by CRDS.

For methyl nitrate photolysis, Talukdar et $al.$ measured a value of $\Phi_{NO_2} = 1.1 \pm 0.3$ at photolysis wavelengths of 248 and 308 nm that was independent of pressure in the range 60 – 700 Torr.[15] Up to 12 Torr of methyl nitrate was used, with UV energies of ≤10 mJ per pulse. Other photochemical pathways for methyl nitrate were shown to have negligible quantum yields. Furthermore, Derro et $al.$ investigated the photodissociation dynamics of methyl nitrate at a wavelength of 193 nm and concluding that the primary photolysis pathway resulted in NO_2 and a CH_3O radical.[30] The UV energies of ≤1.5 mJ per pulse used in the current measurements are lower than for most prior studies, although the photolysis beam profiles are also smaller, and saturation of the $RONO_2$ absorptions is not thought to be significant. The variance-weighted mean of all the data for methyl nitrate obtained at various pressures studied in the current work gives $\Phi_{NO_2} = 1.03 \pm 0.05$ (1 SD).

Ethyl nitrate was previously reported to have a quantum yield for NO_2 formation of unity (1.0 ± 0.1) independent of temperature (278 – 298 K) at 308 nm.[21] The experiments used 1 – 10 Torr of ethyl nitrate and UV photolysis energies from ~20 – 40 mJ per pulse to measure the quantum yield. From the current work, the NO_2 quantum yield from ethyl nitrate photolysis, averaged over all wavelengths and sample pressures used, is $\Phi_{NO_2} = 0.98 \pm 0.09$ (1 SD).

Temperature independent (278 – 298 K) NO_2 quantum yields for n-propyl nitrate and isopropyl nitrate at 308 nm, $\Phi_{NO_2} = 1.0 \pm 0.1$ (for both propyl nitrates) were previously reported by Zhu and Kellis.[22] These prior experiments used alkyl nitrate pressures from 1 – 14 Torr, with ~20 mJ per pulse of UV energy. The primary products of the photodissociation of these alkyl nitrates were therefore NO_2 and an alkoxy radical. From the current work, the corresponding quantum yields (and 1 SD uncertainties) for n-propyl and isopropyl nitrate are $\Phi_{NO_2} = 1.01 \pm 0.04$ and 1.00 ± 0.05, respectively, when averaged over all wavelengths and sample pressures used, in excellent agreement with the results of Zhu and Kellis.

The measurements presented in this work and in previously published studies show that alkyl nitrate photodissociation proceeds predominantly along one reaction pathway, yielding NO_2 and alkoxy radical products via a fast and direct dissociation (or predissociation) process. The length and substitution of the alkyl nitrate has no apparent effect on NO_2 quantum yields

although absorption cross sections differ. The invariance of quantum yields for total $RONO_2$ / N_2 sample pressures in the range 250 – 700 Torr suggests that there is no significant collisional relaxation of the excited state of $RONO_2$ at the higher pressures.

Although comparable studies of photochemical quantum yields for the dinitrates were problematic because of low sample vapour pressures, sufficient pressure of dinitrate A could be generated for NO_2 yield measurements. However, the photolysis experiments performed on dinitrate A give $\Phi_{NO_2} \leq 0.25$, suggesting that dissociation into NO_2 and a radical product is a more minor channel at a photolysis wavelength of 290 nm than for the alkyl (mono) nitrates. To seek some further understanding of the photochemistry of the dinitrate compouds, we carried out calculations of the energies and orbital characters of their electronically excited states. The results are presented in section 3.3.

3.3 Calculations of Electronically Excited States of Dinitrates A and B

To compare the character of the electronically excited states of the dinitrate compounds with those of the mononitrates, we undertook calculations using time dependent density functional theory (TDDFT). We tested both the B3LYP [31-32] and CAM (Coulomb-Attenuating Method)-B3LYP [33] functionals against a coupled cluster method, RICC2 (coupled cluster with approximate singles and doubles and the resolution of identity).[34] Calculations were performed in Gaussian 03[35] and Turbomole[36] programs and used both the Karlsruhe 'def2' (default2) basis set, TZVPP (a triple zeta valence basis augmented by polarization functions[37]) and a Pople type basis set, 6-311G+(d,p).[34] Ground state geometries were optimized with each method and bond dissociation energies computed, and are summarized elsewhere.[38] The optimized ground states were used in TDDFT calculations of vertical excitation energies for the lowest few electronically excited singlet states. Both the ground state geometries and excited state energies were obtained at the same level of theory in calculations using B3LYP/6-311G+(d,p), B3LYP/TZVPP and CAM-B3LYP/TZVPP methods. Selected outcomes are presented here and in Supplementary Information.

The excited states of methyl nitrate were initially investigated as a check of the methodology, because comparisons were possible with previously published calculations.[28, 30, 39] The results are presented in the Supplementary Information, where they are compared with Multistate

CASPT2 calculations from Soto *et al.*[39] The methyl nitrate TDDFT calculations performed using the TZVPP basis set displayed better agreement with these higher level calculations than did those executed using the 6-311+G(d,p) basis set. The following discussion therefore focuses on CAM-B3LYP/TZVPP or B3LYP/TZVPP calculations.

The important transitions predicted in dinitrate A (C_1 symmetry) are presented in Table 2. Dinitrate A contains two NO_2 chromophores, so for each transition (e.g. $\pi^* \leftarrow n$, $\pi^* \leftarrow \pi$) there are two outcomes depending on the NO_2 group associated with the excitation. We label the NO_2 closer to the C=C bond as α and the more remote $-NO_2$ as β. TDDFT is known to have difficulties reproducing energies of charge transfer type transitions,[33, 40-41] but the CAM-B3LYP functional improves the long range interactions of DFT, and so provides a better prediction of charge transfer energies.[33] Only the TDDFT/CAM-B3LYP calculations for the dinitrates are presented here.

Table 2: Dinitrate A (C_1 symmetry) Vertical Excitation Wavelengths (λ) and Oscillator Strengths (*f*) calculated using TDDFT/CAM-B3LYP/TZVPP. α and β respectively refer to excitation of the NO_2 closer to and more distant from the C=C bond. Note that transitions with *f* = 0 can gain some oscillator strength through vibronic coupling.

Transition	Excited State and NO$_2$ group	λ (nm) CAM-B3LYP	*f*
π^* $NO_2 \leftarrow n$ NO_2	S_1 (α)	249	0
	S_2 (β)	248	0
π^* $NO_2 \leftarrow \sigma_{NO}$	S_3 (α)	207	0.0003
	S_4 (β)	206	0.0004
π^* $NO_2 \leftarrow \pi$ C=C	S_5	184	0.059

π^* NO$_2$ $\leftarrow$ $\pi_{D/O}$	S$_6$ (β)	176	0.12
	S$_7$ (α)	173	0.048
π^* C=C $\leftarrow$ π C=C	S$_8$	165	0.14

The Supplementary Information contains plots of the excited molecular orbitals corresponding to the upper states of the transitions listed in Table 2. These plots were generated using Molekel software.[42] The lowest energy transitions in dinitrate A, as with methyl nitrate, are the $\pi^* \leftarrow$ n excitations localised on the NO$_2$ moieties. The energies and oscillator strengths of the corresponding excitations in dinitrate A and methyl nitrate are comparable. There is negligible difference in the $\pi^* \leftarrow$ n transitions originating from the two NO$_2$ moieties. In Table 2, π^* NO$_2$ $\leftarrow$ $\pi_{D/O}$ at shorter wavelength denotes a transition from a non-bonding orbital largely localized on the O atom of the donor R$-$O moiety (π_D) or from orbitals localized on the O atoms of the NO$_2$ group (π_O). Additional transitions in dinitrate A, not found in methyl nitrate, are π^* NO$_2$ $\leftarrow$ π C=C (184 nm) and π^* C=C $\leftarrow$ π C=C (165 nm) but can be neglected in the context of tropospheric photochemistry.

Table 3: Dinitrate B (C_2 symmetry) Vertical Excitation Wavelengths (λ) Calculated Using TDDFT/CAM-B3LYP/TZVPP and RICC2/TZVPP Methods, and Oscillator Strengths (f) from the TDDFT Calculations.

Transition	Excited state	λ (nm)		C_2 Symmetry Type	f
		CAM-B3LYP	RICC2		
π^* NO$_2$ $\leftarrow$ n NO$_2$	S$_1$	255	252	a	0
	S$_2$	255	252	b	0
π^* NO$_2$ $\leftarrow$ σ_{NO}	S$_3$	223	217	b	0.002
	S$_4$	223	217	a	0
π^* NO$_2$ $\leftarrow$ π_D	S$_5$	196	208	b	0.1
	S$_6$	195	208	a	0.01
π^* C=C $\leftarrow$ π C=C	S$_7$	182	175	b	0.5

Table 3 lists calculated transition energies (expressed as wavelengths) and oscillator strengths for dinitrate B. This compound has C_2 symmetry, so each transition can be categorized as either *a* or *b* symmetry type. The longest wavelength transition again involves a $\pi^* \leftarrow n$

excitation localized on the NO_2 moiety. The Table contrasts values obtained using TDDFT/CAM-B3LYP/TZVPP and RICC2/TZVPP methods, with RICC2/T2VPP also used to optimize the ground state geometry in the latter case. The level of agreement supports the choice of TDDFT method used here. Molecular orbital plots are presented in the Supplementary Information.

The analysis of excitations in dinitrates A and B offers no clear rationale for lower quantum yields for photochemical production of NO_2 from dinitrate A because the two NO_2 chromophores behave in the same way as for the mononitrates. Any explanation of our experimental observations for dinitrate A quantum yields must therefore lie in the dynamics that occur after photoexcitation. In methyl nitrate, the first excited state is crossed by a repulsive state, which leads to prompt production of NO_2.[39] Dinitrate A appears to have relaxation pathways that compete with NO_2 loss following absorption of UV light of wavelengths around 300 nm. A quantum yield lower than unity might be explained, at least in part, if the two distinct $-ONO_2$ groups exhibit different dissociation behaviour. If, as our calculations suggest, these nitrate groups act as independent chromophores, with the presence of the carbon-carbon double bond deactivating the closer of the two $-ONO_2$ groups, while the terminal $-ONO_2$ exhibits behaviour typical of alkyl mono-nitrates, a quantum yield of 0.5 would be estimated. However, confirmation (or otherwise) of fast relaxation pathways to the ground state requires a detailed study of the excited and ground state potential energy surfaces involved in the photochemistry. Calculations characterizing the bound and repulsive states in the dinitrates and their intersections are beyond the scope of our current study.

3.4 Atmospheric Photolysis Rate Coefficients

Quantum yields, absorption cross-sections and solar photon flux data were combined to calculate photolysis rate coefficients, J (s^{-1}), using altitude-dependent photon fluxes from the Tropospheric Ultraviolet and Visible (TUV) radiation model for the lower atmosphere (0 – 15 km altitude).[43] The photolysis rate coefficients were calculated for conditions representing Bristol (51°N, 2°W) over the tropospherically relevant wavelength range of 280 – 320 nm in winter (1st January) and summer (1st July). In these calculations, photolysis was considered to be the only significant loss process, so reactive removal by OH radicals, for example, was omitted. The winter J values for methyl, ethyl, n-propyl and isopropyl nitrate

were calculated to be 5.4×10^{-8}, 2.2×10^{-7}, 2.5×10^{-7} and 2.7×10^{-7} s^{-1}, respectively. Likewise, the summer J values were 6.0×10^{-7}, 1.9×10^{-6}, 2.3×10^{-6} and 2.6×10^{-6} s^{-1}. These C_1-C_3 photolysis rate coefficient estimates are in good agreement with previous studies.[13, 18-19, 25, 44]

4. Conclusions

The quantum yields for photochemical production of NO_2 from various alkyl nitrates are shown to be unity within experimental uncertainties at wavelengths of 290 – 315 nm, and independent of the pressure of (excess) N_2 at total sample pressures from 250 – 700 Torr. Ultraviolet absorption cross sections for 240 nm $\leq \lambda \leq$ 320 nm agree well with previous reports. Tropospheric rates of photolysis of $RONO_2$ and consequent release of NO_2 will be controlled by these cross sections and quantum yields for wavelengths $\geq$290 nm. Our measurements of quantum yields for NO_2 from photolysis of an unsaturated dinitrate (but-3-ene-1,2-diyl dinitrate) suggest an upper limit of $\Phi_{NO_2} = 0.25$, although the experimental measurements are made difficult by the low vapour pressure of the parent compound.

Supporting Information Available

The Supporting Information contains tables of absorption cross section values (and uncertainties) for gaseous methyl, ethyl, n-propyl and isopropyl nitrate and for acetonitrile solutions of ethyl nitrate, isopropyl nitrate, but-3-ene-1,2-diyl dinitrate and (Z)-but-2-ene-1,4-diyl dinitrate (dinitrates A and B). Beam waists for the UV photolysis laser are tabulated for the photolysis wavelengths used. Infra-red and NMR spectral data are reported for all the

synthesized organic nitrates. TDDFT CAM-B3LYP calculations of vertical excitation energies and oscillator strengths for methyl nitrate are compared to previously reported calculations, and orbital plots are presented for the excited electronic states of dinitrates A and B. The information is available free of charge via the Internet at http://pubs.acs.org.

References

1.   Atkinson, R.; Arey, J., Gas-Phase Tropospheric Chemistry of Biogenic Volatile Organic Compounds: A Review. *Atm. Env.* **2003,** *37*, S197-S219.
2.   Roberts, J. M., The Atmospheric Chemistry of Organic Nitrates. *Atm. Environ.* **1990,** *24*, 243-287.
3.   Roberts, J. M.; Fajer, R. W., UV Absorption Cross-Sections of Organic Nitrates of Potential Atmospheric Importance and Estimation of Atmospheric Lifetimes. *Environ. Sci. Technol.* **1989,** *23*, 945-951.
4.   Perring, A. E.; Bertram, T. H.; Wooldridge, P. J.; Fried, A.; Heikes, B. G.; Dibb, J.; Crounse, J. D.; Wennberg, P. O.; Blake, N. J.; Blake, D. R., et al., Airborne Observations of Total $RONO_2$: New Constraints on the Yield and Lifetime of Isoprene Nitrates. *Atm. Chem. Phys.* **2009,** *9*, 1451-1463.
5.   Blake, N. J.; Blake, D. R.; Swanson, A. L.; Atlas, E.; Flocke, F.; Rowland, F. S., Latitudinal, Vertical, and Seasonal Variations of C_1-C_4 Alkyl Nitrates in the Troposphere over the Pacific Ocean During PEM-Tropics A and B: Oceanic and Continental Sources. *J. Geophys. Res.-Atm.* **2003,** *108*, 8242 (1-13).
6.   Simpson, I. J.; Meinardi, S.; Blake, D. R.; Blake, N. J.; Rowland, F. S.; Atlas, E.; Flocke, F., A Biomass Burning Source of C_1-C_4 Alkyl Nitrates. *Geophys. Res. Lett.* **2002,** *29*.
7.   Barnes, I.; Becker, K. H.; Zhu, T., Near UV Absorption-Spectra and Photolysis Products of Difunctional Organic Nitrates - Possible Importance as NO(X) Reservoirs. *J. Atm. Chem.* **1993,** *17*, 353-373.
8.   Beaver, M. R.; St Clair, J. M.; Paulot, F.; Spencer, K. M.; Crounse, J. D.; LaFranchi, B. W.; Min, K. E.; Pusede, S. E.; Wooldridge, P. J.; Schade, G. W., et al., Importance of Biogenic Precursors to the Budget of Organic Nitrates: Observations of Multifunctional Organic Nitrates by CIMS and TD-LIF During Bearpex 2009. *Atm. Chem. Phys.* **2012,** *12*, 5773-5785.
9.   Farmer, D. K.; Perring, A. E.; Wooldridge, P. J.; Blake, D. R.; Baker, A.; Meinardi, S.; Huey, L. G.; Tanner, D.; Vargas, O.; Cohen, R. C., Impact of Organic Nitrates on Urban Ozone Production. *Atm. Chem. Phys.* **2011,** *11*, 4085-4094.
10.   Barnes, I.; Bastian, V.; Becker, K. H.; Tong, Z., Kinetics and Products of the Reactions of Nitrate Radical with Monoalkenes, Dialkenes, and Monoterpenes. *J. Phys. Chem.* **1990,** *94*, 2413-2419.
11.   Perring, A. E.; Wisthaler, A.; Graus, M.; Wooldridge, P. J.; Lockwood, A. L.; Mielke, L. H.; Shepson, P. B.; Hansel, A.; Cohen, R. C., A Product Study of the Isoprene+NO_3 Reaction. *Atm. Chem. Phys.* **2009,** *9*, 4945-4956.
12.   Rollins, A. W.; Kiendler-Scharr, A.; Fry, J. L.; Brauers, T.; Brown, S. S.; Dorn, H. P.; Dube, W. P.; Fuchs, H.; Mensah, A.; Mentel, T. F., et al., Isoprene Oxidation by Nitrate Radical: Alkyl Nitrate and Secondary Organic Aerosol Yields. *Atm. Chem. Phys.* **2009,** *9*, 6685-6703.

13.   Clemitshaw, K. C.; Williams, J.; Rattigan, O. V.; Shallcross, D. E.; Law, K. S.; Cox, R. A., Gas-Phase Ultraviolet Absorption Cross-Sections and Atmospheric Lifetimes of Several C_2-C_5 Alkyl Nitrates. *J. Photochem. Photobiol. A* **1997,** *102*, 117-126.

14.   Talukdar, R. K.; Herndon, S. C.; Burkholder, J. B.; Roberts, J. M.; Ravishankara, A. R., Atmospheric Fate of Several Alkyl Nitrates .1. Rate Coefficients of the Reactions Alkyl Nitrates with Isotopically Labelled Hydroxyl Radicals. *J. Chem. Soc. Faraday Trans.* **1997,** *93*, 2787-2796.

15.   Talukdar, R. K.; Burkholder, J. B.; Hunter, M.; Gilles, M. K.; Roberts, J. M.; Ravishankara, A. R., Atmospheric Fate of Several Alkyl Nitrates .2. UV Absorption Cross-Sections and Photodissociation Quantum Yields. *J. Chem. Soc. Faraday Trans.* **1997,** *93*, 2797-2805.

16.   Luke, W. T.; Dickerson, R. R.; Nunnermacker, L. J., Direct Measurements of the Photolysis Rate Coefficients and Henry Law Constants of Several Alkyl Nitrates. *J. Geophys. Res.-Atm.* **1989,** *94* (D12), 14905-14921.

17.   Taylor, W. D.; Allston, T. D.; Moscato, M. J.; Fazekas, G. B.; Kozlowski, R.; Takacs, G. A., Atmospheric Photo-Dissociation Lifetimes for Nitromethane, Methyl Nitrite, and Methyl Nitrate. *Int. J. Chem. Kinet.* **1980,** *12*, 231-240.

18.   Shallcross, D. E.; Biggs, P.; CanosaMas, C. E.; Clemitshaw, K. C.; Harrison, M. G.; Alanon, M. R. L.; Pyle, J. A.; Vipond, A.; Wayne, R. P., Rate Constants for the Reaction between OH and CH_3ONO_2 and $C_2H_5ONO_2$ over a Range of Pressure and Temperature. *J. Chem. Soc. Faraday Trans.* **1997,** *93*, 2807-2811.

19.   Gorrotxategi Carbajo, P.; Orr-Ewing, A. J., NO_2 Quantum Yields from Ultraviolet Photodissociation of Methyl and Isopropyl Nitrate. *Phys Chem Chem Phys* **2010,** *12*, 6084-6091.

20.   Luke, W. T.; Dickerson, R. R., Direct Measurements of the Photolysis Rate Coefficient of Ethyl Nitrate. *Geophys. Res. Lett.* **1988,** *15*, 1181-1184.

21.   Zhu, L.; Ding, C. F., Temperature Dependence of the near UV Absorption Spectra and Photolysis Products of Ethyl Nitrate. *Chem. Phys. Lett.* **1997,** *265*, 177-184.

22.   Zhu, L.; Kellis, D., Temperature Dependence of the UV Absorption Cross Sections and Photodissociation Products of C_3-C_5 Alkyl Nitrates. *Chem. Phys. Lett.* **1997,** *278*, 41-48.

23.   Blatt, A. H., *Organic Syntheses*. John Wiley and Sons: New York, 1943; Vol. 2.

24.   ChemSpider. http://www.chemspider.com/.

25.   Turberg, M. P.; Giolando, D. M.; Tilt, C.; Soper, T.; Mason, S.; Davies, M.; Klingensmith, P.; Takacs, G. A., Atmospheric Photochemistry of Alkyl Nitrates. *J. Photochem. Photobiol. A* **1990,** *51*, 281-292.

26.   Rattigan, O.; Lutman, E.; Jones, R. L.; Cox, R. A.; Clemitshaw, K.; Williams, J., Temperature-Dependent Absorption Cross-Sections of Gaseous Nitric-Acid and Methyl Nitrate. *J. Photochem. Photobiol. A* **1992,** *66*, 313-326.

27.   Csizmadia, V. M.; Houlden, S. A.; Koves, G. J.; Boggs, J. M.; Csizmadia, I. G., Stereochemistry and Ultraviolet Spectra of Simple Nitrate Esters. *J. Org. Chem.* **1973,** *38*, 2281-2287.

28.   Harris, L. E., Lower Electronic States of Nitrite and Nitrate Ion, Nitromethane, Nitramide, Nitric-Acid, and Nitrate Esters. *J. Chem. Phys.* **1973,** *58*, 5615-5626.

29.   Vandaele, A. C.; Hermans, C.; Fally, S.; Carleer, M.; Colin, R.; Merienne, M. F.; Jenouvrier, A.; Coquart, B., High-Resolution Fourier Transform Measurement of the NO_2 Visible and near-Infrared Absorption Cross Sections: Temperature and Pressure Effects. *J Geophys Res-Atmos* **2002,** *107* (D18), 4348.

30.   Derro, E. L.; Murray, C.; Lester, M. I.; Marshall, M. D., Photodissociation Dynamics of Methyl Nitrate at 193 nm: Energy Disposal in Methoxy and Nitrogen Dioxide Products. *Phys. Chem. Chem. Phys.* **2007,** *9*, 262-271.

31.   Becke, A. D., *J. Chem. Phys.* **1993,** *98*, 5648-5652.

32.   Stephens, P. J.; Devlin, F. J.; Chabalowski, C. F.; Frisch, M. J., *J. Phys. Chem.* **1994,** *98*, 11623-11627.

33.   Yanai, T.; Tew, D. P.; Handy, N. C., A New Hybrid Exchange-Correlation Functional Using the Coulomb-Attenuating Method (CAM-B3LYP). *Chem. Phys. Lett.* **2004,** *393*, 51-57.

34.   Jensen, F., *Introduction to Computational Chemistry*. Second ed.; Wiley-Blackwell: Chichester, UK, 2007.

35.   Frisch, M. J.; Trucks, G. W.; Schlegel, H. B.; Scuseria, G. E.; Robb, M. A.; Cheeseman, J. R.; Montgomery, J. A.; Vreven, T.; Kudin, K. N.; Burant, J. C., et al., *Gaussian 03*, 2003.

36.   TURBOMOLE V5.10, 2008; Available at:http://www.turbomole.com.

37.   Weigend, F.; Ahlrichs, R., Balanced Basis Sets of Split Valence, Triple Zeta Valence and Quadruple Zeta Valence Quality for H to Rn: Design and Assessment of Accuracy. *Phys. Chem. Chem. Phys.* **2005,** *7*, 3297-3305.

38.   Higgins, C. M. Tropospheric Photochemistry of Organic Nitrates. University of Bristol, 2013.

39.   Soto, J.; Pelaez, D.; Otero, J. C.; Avila, F. J.; Arenas, J. F., Photodissociation Mechanism of Methyl Nitrate. A Study with the Multistate Second-Order Multiconfigurational Perturbation Theory. *Phys. Chem. Chem. Phys.* **2009,** *11*, 2631-2639.

40.   Dreuw, A.; Weisman, J. L.; Head-Gordon, M., Long-Range Charge-Transfer Excited States in Time-Dependent Density Functional Theory Require Non-Local Exchange. *J. Chem. Phys.* **2003,** *119*, 2943-2946.

41.   Tozer, D. J.; Amos, R. D.; Handy, N. C.; Roos, B. O.; Serrano-Andres, L., Does Density Functional Theory Contribute to the Understanding of Excited States of Unsaturated Organic Compounds? *Mol. Phys.* **1999,** *97*, 859-868.

42.   Varetto, U. *Molekel 5.4*, Swiss National Supercomputing Centre, Lugano.

43.   Tropospheric Ultraviolet and Visible Model. http://cprm.acd.ucar.edu/Models/TUV/.

44.   Bottenheim, J. W.; Barrie, L. A.; Atlas, E., The Partitioning of Nitrogen-Oxides in the Lower Arctic Troposphere During Spring 1988. *J. Atm. Chem.* **1993,** *17*, 15-27.

Table of Contents Graphic